Chaos evidence in catecholamine secretion at chromaffin cells[☆]

G. Quiroz[1*], I. Bonifas[2], J.G. Barajas-Ramirez[2], R. Femat[2].

[1] *Facultad de Ingeniería Mecánica y Eléctrica, Centro de Innovación Investigación y Desarrollo en Ingeniería y Tecnología, UANL, Pedro de Alba s/n, San Nicolás de los Garza, N.L. México.*

[2] *Laboratorio para la Biodinámica y Sistemas Alineales, División de Matemáticas Aplicadas, IPICyT, Camino a la Presa de San José 2055, San Luis Potosí, S. L. P. México.*

Abstract

Chromaffin cells secrete catecholamine molecules via exocytosis process. Each exocytotic event is characterized by a current spike, which corresponds to the amount of released catecholamine from secretory vesicles after fusing to plasma membrane. The current spike might be measured by the oxidation of catecholamine molecules and can be experimentally detected through amperometry technique. In this contribution, the secretion of catecholamine, namely adrenaline, of a set of bovine chromaffin cells is measured individually at each single cell. The aim is to study quantitative results of chaotic behavior in catecholamine secretion. For analysis, time series were obtained from amperometric measurements of each single chromaffin cell. Three analysis techniques were exploited: i) a low-order attractor was generated by means of phase space reconstruction, Average Mutual Information (AMI) and False Nearest Neighbors (FNN) were used to compute embedding lag and embedding dimension, respectively. ii) The properties of power spectrum density of time series were studied by Fast Fourier Transform (FFT) looking for possible dominant frequencies in power spectrum. iii) Maximun Lyapunov Exponent (MLE) analysis was done to study the divergence of trajectories of the time series. Nevertheless, in order to dismiss the possibility of positiveness of MLE are due to the inherent noise in experiments, seven surrogate data sets computed using the Amplitude Adjusted Fourier Transform (AAFT) algorithm was computed. The phase space reconstruction showed that, in all cases, the trajectories lie in an embedding subspace suggesting oscillatory nature. The FFT analysis showed high dispersion of the power spectrum without any predominant frequency range. MLE analysis showed that the MLE values are positive for a given orbit time and a

[☆]This research was supported by CONACYT under grants 48307-R and 84962-J2.

[*]Corresponding author.

Email addresses: griselda.quirozcm@uanl.edu.mx (G. Quiroz[1]), imelda@ipicyt.edu.mx (I. Bonifas[2]), jgbarajas@ipicyt.edu.mx (J.G. Barajas-Ramirez[2]), rfemat@ipicyt.edu.mx (R. Femat[2].)

defined range of maximum scale values. Moreover, the trajectory of the MLE evolution of all the surrogate data are asymptotic and hold positive along the maximum scale range. These findings are preliminary evidence on detecting chaotic behavior in catecholamine secretion and, in general, their provide a first step towards a deeply understanding of nonlinear behavior of protein releasing dynamics.

Key words: Dynamics in biosystems, Chromaffin cells, Catecholamine secretion, Exocytosis.

---

1. Introduction

Catecholamine molecules are biologically active products, as neurotransmitters and hormones, of a neuroendocrine system called sympathochromaffin [1]. The sympathochromaffin system is a versatile communication system whose neural effects are almost instantaneous, hormonal effects are perceptible in few minutes [2], and includes two elements: sympathetic nervous system and chromaffin tissues. Sympathetic nervous system innervates chromaffin tissue via sympathetic preganglionic neurons, which belong to sympathetic efferents of the Autonomic Nervous System. The major clusters of chromaffin cells are in adrenal medulla, which also is innervated by preganglionic neurons. There are three main types of catecholamines: adrenaline, noradrenaline and dopamine. All of them are secreted directly into the circulation by chromaffin cells. The secretion process of catecholamine molecules is exocytosis, which is a key process in synaptic transmission in the brain, in neuromuscular junctions and into the blood by chromaffin cells from the adrenal gland [3]-[8].

There exist a wide number of biological effects induced by catecholamines [9]. In hemodynamics, the effect of catecholamines in vasoconstriction, vasodilatation, and increase in the rate and force of myocardial contraction. In particular, noradrenaline causes generalized vasoconstriction and an increase in systolic and diastolic pressure. Adrenaline causes vasoconstriction in, among others, skin, kidney, and mucosae. Also, adrenaline causes vasodilatation in others organs, for example in skeletal muscle, and increments in hepatic blood flow, heart rate, cardiac output, and systolic blood pressure. Dopamine causes increment in cardiac output. In metabolism, the catecholamine produces multiples indirect and direct effects. Indirect effects are related to changes on the hormonal secretion; for example, on both suppression and stimulation of insulin release. Some of the major direct effects involve stimulation of hepatic glucose production (glyconeogenesis and glycogenolysis) and release of amino acids from muscle [9].

Causes and effects of catecholamine secretion form a highly complex system where different kind of physiological processes are involved. The complexity of catecholamine secretion and its role in crucial physiological functions draw up it as an attractive phenomenon of study. Besides improving comprehension of how catecholamine secretion is carried out, dynamical analysis can open new interesting questions about this phenomenon, for instance: Is catecholamine

secretion a deterministic phenomenon?, Is the catecholamine secretion a phenomenon governed by noise? or Is phenomenon of catecholamine secretion a structured disorder? This kind of questions have already arisen in other systems of neurotransmitter release. For example, in vertebrate neuromuscular junctions, the oscillatory nature of neurotransmitter release has been widely studied [10]-[13]. Such oscillations are related to presynaptic factors, such as the concentration of calcium ions in the extracellular medium and inside the nerve terminal, the polarization of the nerve membrane, and the metabolic state of the nerve terminal [14]-[19]. Also, the deterministic nature of these oscillations has been corroborated from a nonlinear analysis [20].

In contrast with previous approaches, in this contribution, we use measured data from amperometry in a single mammal chromaffin cell to study the dynamic behavior of catecholamine secretion. The main difference of mammal chromaffin cells respect to neuromuscular junctions is that, in the former, there is an usual unique active zone and, in the latter, there are a large number of active zones. Thus, we study the dynamics of the adrenaline secretion in single chromaffin cells. Each cell was stimulated by a Ba^{2+} solution during 10 s and adrenaline secretion was measured by amperometry around 400 s. Nonlinear analysis is implemented on time series of measurements resulting from exocytotic events. We seek evidence about chaotic behavior in exocytosis phenomenon. The document is organized as follows: in the next section, a brief summary of catecholamine secretion and amperometry technique is given, describing the experimental setup for catecholamine measurements. In Section 3, a phase space reconstruction is shown, considering Average Mutual Information (AMI) analysis and False Nearest Neighbor (FNN) in order to compute embedding lag and embedding dimension. Also, power spectrum analysis, and computation of Maximum Lyapunov Exponent (MLE) are shown. Finally, we show some concluding remarks.

2. Measurement protocol

Electrochemical analysis of the secretion of neurotransmitters with untramicroelectrodes has allowed the quantification of these events with the precision required to propose and soundly validate quantitative kinetic physicochemical models [21, 24]. A voltametric analysis of the nature of neurotransmitters was introduced by the group of R.M Wightman [22, 23]. Secretion of neurotransmitters is detected as a series of current spikes that correspond to the detection of concentration pulses generated by exocytosis. The use of carbon fiber ultramicroelectrodes to measure and identify the chemical signaling of neurotransmitters has provided a main advance in the study into cell communication. Electrochemical techniques provide the unique opportunity to examine the effect of chemical and physical parameters on both the rate of secretion and quantity of material extruded from the vesicles. In view of the larger size of proteins, neurotransmitters diffuse very rapidly since they are relatively very small and are easily oxidized via electrochemical methods. For example, acetylcholine is a vital part of the neural transport system in mammalians and is easy to be

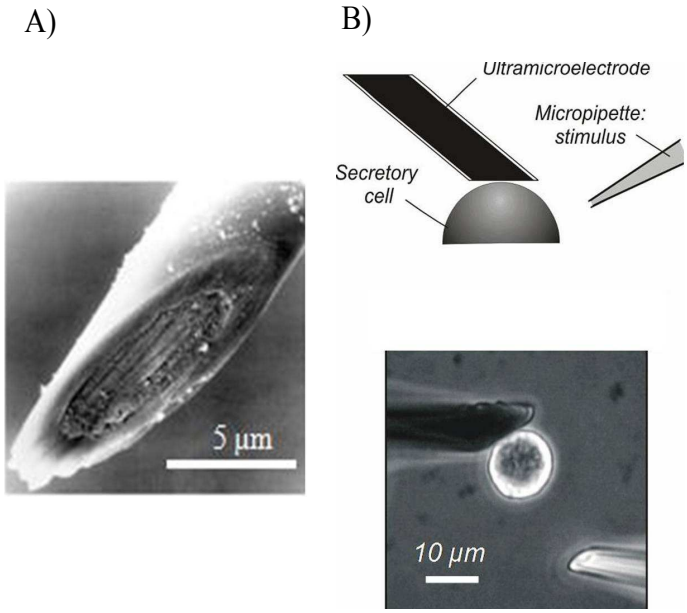

Figure 1: A) Electron microscopy micrograph of a microelectrode where the carbon fiber is coated with a thin Nafion film after polishing at an angle of 45 . B) Experimental arrangement for exocytosis detection on chromaffin cells. A diagram of each part of the process is shown in the top. In the bottom, a microscopic view of the microelectrode tip is observed on the left side of the photography, in close contact with the chromaffin cell stimulated by a barium ion solution (BaCl2 2 mM) injected through a micropipette, positioned on the low right side of the cell.

oxidized. It is chemical rather than biochemical in size as well as other catecholamines neuromediators such as adrenaline or dopamine.

In electrochemical methods the ultramicroelectrode (a thin carbon fiber shown in Figure 1A) is the central transducer which allow us to study, detecting and quantifying the release of neurotransmitters which characterize the phenomenon of exocytosis. The precise positioning of an ultramicroelectrode at micrometric distances from an isolated living secretory cell ensures that selected electroactive materials released by the cell can be collected (over a millisecond time scale) and analyzed by the electrode surface, reflecting precisely the cellular release kinetics [25]-[27]. An experimental arrangement for exocytosis detection on chromaffin cells is shown in Figure 1B.

As we mentioned before, electrochemical measurements of the rate of neurotransmitters secretion with ultramicroelectrodes allowed to quantify these events with the precision required to propose and validate physicochemical models that might rationalize their occurrence. In this sense, the precise positioning of an ultramicroelectrode at micrometric distances from an isolated living cell (neuron, chromaffin, mast or pancreatic cell, fibroblast, macrophage) [25, 27, 28] ensures that selected electroactive material released by the cell can be collected

and analyzed by the electrode surface, reflecting precisely the cellular release kinetics. Indeed, the film of extracellular fluid comprised between the cell and the electrode surfaces defines an artificial synaptic cleft of a few hundred femtoliters volume, in which the release of minute molecular amounts of chemicals, typically in the range of zepto- to attomoles, produces a sudden and significant concentration rise. This guarantees the detection of the released species with an extremely high signal-to-noise ratio, as well as the determination of the instant released fluxes since the collection efficiency is quantitative. In other words, the assembly cell / liquid cleft / ultramicroelectrode behaves as an artificial synapse and the ultramicroelectrode current mirrors precisely the released fluxes.

Based on this artificial synapse method, carbon fiber ultramicroelectrodes were used to monitor the kinetics of exocytosis of adrenaline by chromaffin cells. Adrenaline molecules that diffuse away from the cell are electrooxidized (two electrons per molecule, [28]) at the surface of the ultramicroelectrode and their flux, $\frac{dN(t)}{dt}$, where $N(t)$ is the number of catecholamine molecules emitted at the time t, this is converted electrochemically into a current $I(t)$ according to the Faraday's law: $I(t) = 2F\frac{dN(t)}{dt}$, where F is the Faraday constant.

The variation of the amperometric current with time is thus a precise kinetic measurement of the catecholamine efflux with a precision in the range of one thousand molecules per millisecond. The dynamics of vesicular release are evidenced by the shape of the current spikes. Thus, the temporal resolution and sensitivity of amperometry for measuring actual secretory transmitters has made it well suited for probing fusion and postfusion events in exocytosis. An example of a continuous experimental amperometric trace showing a succession of individual exocytotic events detected after the stimulation of secretion by a chromaffin cell is shown in Figure 2.

The amperometric monitoring of release through the oxidation of adrenaline molecules (2 e/molecule at E=+650 mV vs. $Ag/AgCl$) provides a succession of spikes, each one corresponding to a single vesicular exocytotic event [29] as is shown in Figure 2A. Electrode placed in contact with the cell and 2mM Ba^{2+} injection during 10 s at 250 hPa under isotonic (315 mOsm) conditions. A typical spike extracted from the trace are enlarged in the amperometric monitoring (see Figure 2B) with a sketch showing the traces without and with a discernable foot preceding the spike (dotted line in the spike's bottom). The type of foot-shape showed by dotted line represents a current that can be stabilized as a plateau curring after its initial rising phase. The spikes extracted from the amperometric trace showing a pre-spike feature observed on about 30% of the amperometric events, which is related to the release through the initial fusion pore. A schematic representation of the main phases of exocytosis (I-V) during full fusion of dense core vesicles with cell membrane is shown at the bottom of Figure 2B. Following the cell stimulation, some vesicles are primed to effect exocytosis (I) and dock to the cell membrane. After the formation of a fusion pore, catecholamine begin to diffuse out of the vesicular matrix through the pore (II). When the surface tension of the vesicle membrane becomes high enough to disrupt the fusion pore structure, full fusion of the vesicle and cell membranes

occurs (III). This process continues up to the point where the vesicular matrix is fully exposed to the extracellular fluid and its content is released (IV-V).

The studies of exocytosis described in this manuscript were conducted on bovine chromaffin cells that control the release of adrenaline and noradrenaline in blood following physiological stresses. Results described in the manuscript were obtained exclusively from single cell experiments. Experimental setup for measurements is as follows.

- **Cell Culture:** Bovine chromaffin cells were prepared by collagenase digestion of the medulla of adrenal glands obtained from a slaughterhouse (Meaux, France). Cells were purified and cultured using previously described methods (see [30]). In brief, purified chromaffin cells were plated at a density of 4×10^4 cells/cm^2 on collagen-poly-L-lysine coated glass coverslips placed in 24 wells plates and incubated in a 5% CO_2 atmosphere at 37°C. Cells were used on days 3 to 7 after culture and 24 hours maximum after plating.

- **Electrode Preparation:** Carbon fiber ultramicroelectrodes (7-μm diameter, Thornel-Cytec Carbon Fibers, Greenville, SC) were constructed as described in [31] and back-filled with mercury. Electrode tips were polished at a 45° angle on a diamond dust-embedded micropipette beveling wheel (Model EG-4, Narishige Co., London, UK) for 10-20 min before experiments. Only electrodes with a very stable amperometric baseline current were used for cell measurements.

- **Measurement preparation:** Each cell was placed coverslip into a 35 mm plastic dish filled with 5 mL of isotonic physiological saline (154 mM $NaCl$, 4.2 mM KCl, 0.7 mM $MgCl_2$, 11.2 mM glucose, 10 mM $HEPES$, pH 7.4). After positioning the dish onto the stage of an inverted microscope (Axiovert-135, Carl Zeiss, Germany), the working electrode was gently lowered onto a single cell using a micromanipulator (Model MHW-103, Narishige Co., London, UK). The close proximity of the electrode polished surface to the cell surface was confirmed by a slight deformation in the outline of the cell. Exocytosis was stimulated by a 10 s barium solution ($BaCl_2$ 2mM in Locke buffer supplemented with 0.7 mM $MgCl_2$, without carbonates) injection from a 20-30 μm diameter glass microcapillary and 250 hPa pulse of barium ion solution (model Femtojet, Eppendorf Inc., Hamburg, Germany). All experiments were performed at 25 ± 2°C.

- **Data Acquisition:** Electrodes were held at + 0.65 V vs. a silver/silver chloride reference electrode using a commercially available picoamperometer (model AMU 130, Radiometer Analytical Instruments, Copenhagen, DK), whose the adjustable time-response was set at 0.5 ms. The output was digitized at 10 to 40 kHz, displayed in real time and stored on a computer (Powerlab 4SP A/D converter and software Chart, AD instruments, Colorado Springs, CO) with no subsequent filtering.

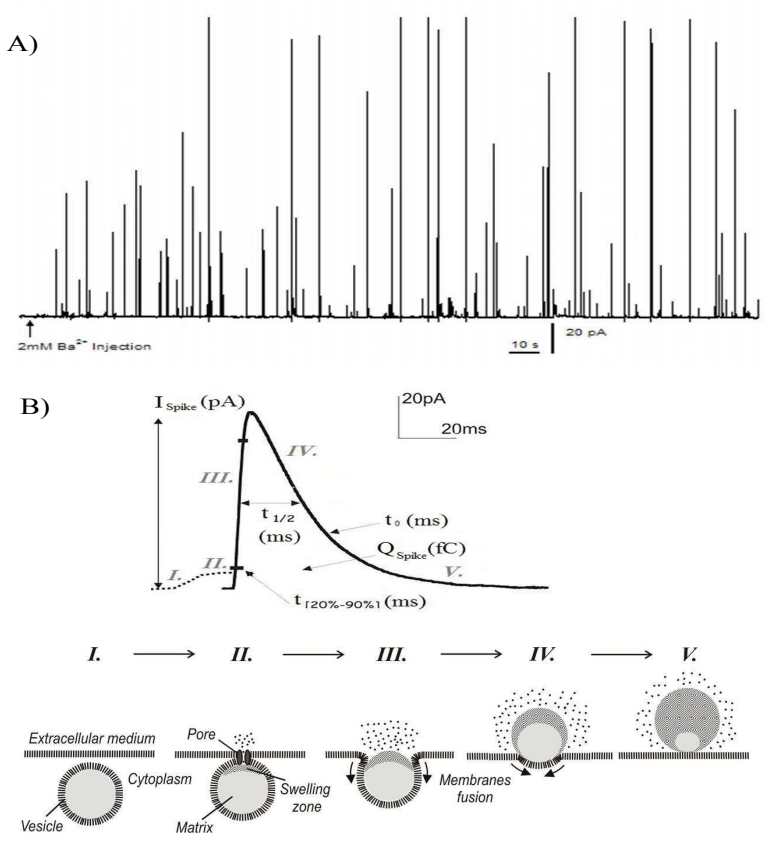

Figure 2: A) The amperometric monitoring of releases through the oxidation of adrenaline molecules (2 e/molecule at E=+650 mV vs. Ag/AgCl) provides a succession of spikes, each one corresponding to a single vesicular exocytotic event [29]. B) A typical spike extracted from the trace is enlarged with a sketch showing a pre-spike feature (dotted line in the bottom of spike) observed on about 30% of the amperometric events, which is related to the release through the initial fusion pore. The schematic representation of the main spike features: maximum oxidation current I_{spike} (pA); total electrical charge Q_{spike} (fC); the half-width $t_{1/2}$ (ms) decomposed into t_1 and t_2; rise time t_{20-90} (the delay between $I = 20$ % of I_{spike} and $I = 90$ % of I_{spike} in ms); mean diffusion time t_0 in amperometric spikes are indicated. The different phases of the exocytosis are identified by their labels I-V.

These experiments were conducted under control conditions, i.e., following a commonly used protocol, where a single chromaffin cell is stimulated for 10 s by a 2 Mm barium ion solution, without any previous or further modification of the cells or of the medium used for measurements. Each amperometric trace from chromaffin cell response during the elapsed time of stimulation was visually inspected and signals were designated as spikes if their maximum current values were 3 times higher than the RMS noise (0.5 to 0.7 pA) of the baseline current (30 ms minimum time-length) recorded prior to each signal. Special attention was applied to verify the baseline stability before and after each spike in order to avoid spike superimposition.

3. Temporal behavior in catecholamine secretion

The time series to be analyzed were obtained from experimental measurements of adrenaline secretion via amperometry. A large number of adrenaline secretion experiments from a single chromaffin cell were recorded in order to analyze the dynamical properties of the exocytotic event. Figure 3 shows three representative time series of the amperometry record of adrenaline secretion in a single chromaffin cell.

3.1. Phase space reconstruction

In the study of time series, time delay embedding analysis is often used to reconstruct the phase space of a dynamical system. An advantage of this technique is that it only requires scalar measurement data, as the dynamical properties of the system under study are established directly from a time series in terms of the obtained delay coordinates [32, 33, 34].

State space reconstruction allows one to visualize the trajectories embedded on a chaotic attractor. Three scenarios are possible: i) if the trajectories converge to an equilibrium, they are not contained in a chaotic attractor; ii) if trajectories converge to stable periodic orbits, chaos will not be exhibited at the reconstructed space; iii) if trajectories describe unstable periodic orbits and remain bounded, is possible that they be contained in a chaotic attractor. In this way, phase space reconstruction, although not a conclusive criterium to demonstrate chaos, is a powerful complementary element towards the inference of chaotic behavior.

In this study, such technique is used to reconstruct an attractor from the amperometric measurements of adrenaline secretion for each time series in Figure 3. According to Taken's theorem for a time series generated by a finite dimensional dynamical system, the existence of an attractor implies the existence of an underlying embedding state space in delay coordinates. Suitable values for the embedding lag (T) and dimension (m) are unknowns that need to be determine from the time series data. Unfortunately, there is no method to determine their optimal values. However, good approximations can be obtained exploiting the deterministic nature of the underlining system [34, 35]. The recommended methodology to determine a suitable embedding dimension is to use

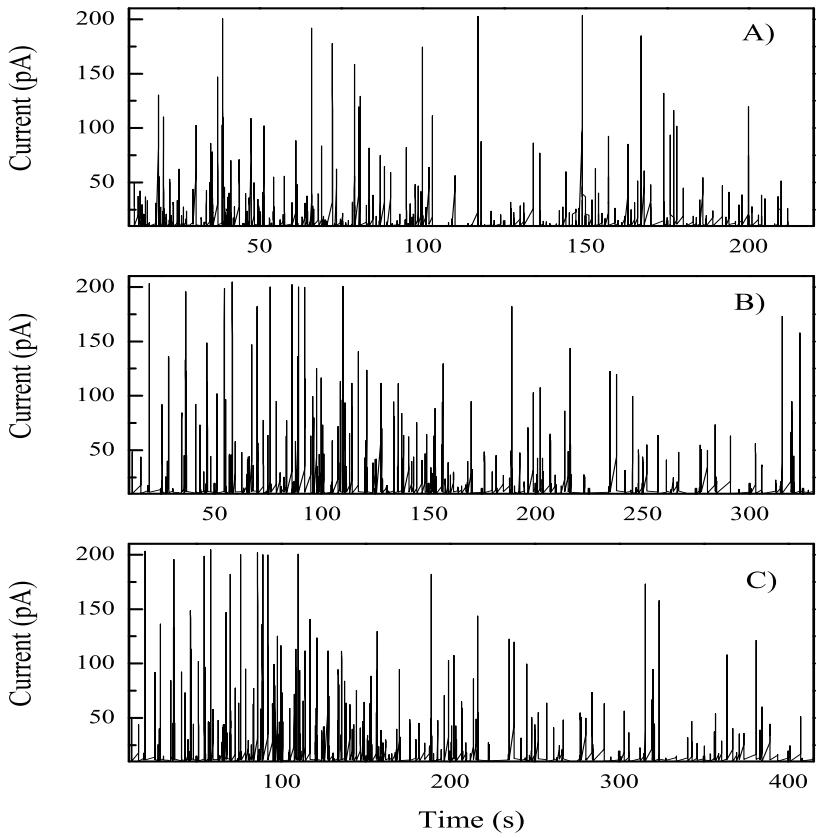

Figure 3: Time series of adrenaline molecules secretion. A), B) and C) show the amperometric measurements of three different experiments, under control conditions, where a single chromaffin cell was stimulated by a barium ion solution. Note the differences in time scale at each time series.

successively higher dimensions and chose the lowest embedding dimension for which the data shows features of deterministic behavior. The most commonly used method to identify signatures of deterministic behavior is the False Nearest Neighbors (FNN) algorithm, the basic idea of the method is to eliminate ambiguity on the reconstructed state space, then, for each embedding dimension, the neighbors of a given point are identified; then if increasing the embedding dimension, this neighbors move faraway, these were false neighbors, and the trajectory needs a higher dimension to be represented without ambiguity.

As to the choice of the embedding lag, theoretically any value of T is acceptable. However, the appearance of the reconstructed attractor depends strongly on the choice of embedding lag, a suitable value for T must separate sufficiently the data in the time series as to have a smooth reconstruction of the attractor, therefore its value must be as large as possible. On the other hand, the lag must not be too large, to avoid deluding the relation that one point in the reconstructed trajectory has with the next. In this sense, a useful measure to establish T is to take the value for which the Average Mutual Information (AMI) has its first minimum. The AMI criterion estimates the among of information about the sample at time $t_o + T$ that is available in the current sample [36]. From the time series, an embedding is constructed using the time-delay state vectors $z(t)$ given by: $z(t) = [x(t), x(t-T), x(t-2T), ..., x(t-(m-1)T)]$. After evaluating AMI and FNN (see Figure 4), the embedding lag and dimension are chosen to be $m = 4$ and $T = 60$ ms. This methodology using AMI and FNN analysis to propose embedding lag and embedding dimension has been widely used for detecting chaos in biomedical signals, for example, biomedical signals involved in human gait [37] or human electrocardiogram [38], and in general, in physical signals [39, 40].

So, for each time series in Figure 3 a reconstructed phase space is presented, the corresponding three-dimensional projections of their resulting reconstructed attractors are shown in Figure 5, along with their projections onto two-dimensional canonical planes. The reconstructed phase space shows that the trajectories are contained in a bounded subspace, implying significant indications of existence of embedding attractors, as well as structured disorder in dynamics of catecholamine secretion, and also possible chaotic behavior. Next, the Fourier spectrum is computed from time series in order to verify frequency and power of oscillations associated to the trajectories in the reconstructed attractors. Previously, an issue is interesting to be remarked: as discussed above, the noise effects on the measurements are minimized by the use of well-established experimental techniques of amperometry, ensuring that the assembly cell/liquid cleft/ultramicroelectrode behave as an artificial synapse and the ultramicroelectrode current mirrors precisely the released fluxes; as well as selecting electrodes with a very stable amperometric baseline current, and considering as spikes that ones which maximum current values were 3 times higher than the RMS noise (0.5 to 0.7 pA) of the baseline current (30 ms minimum time-length) recorded prior to each signal.

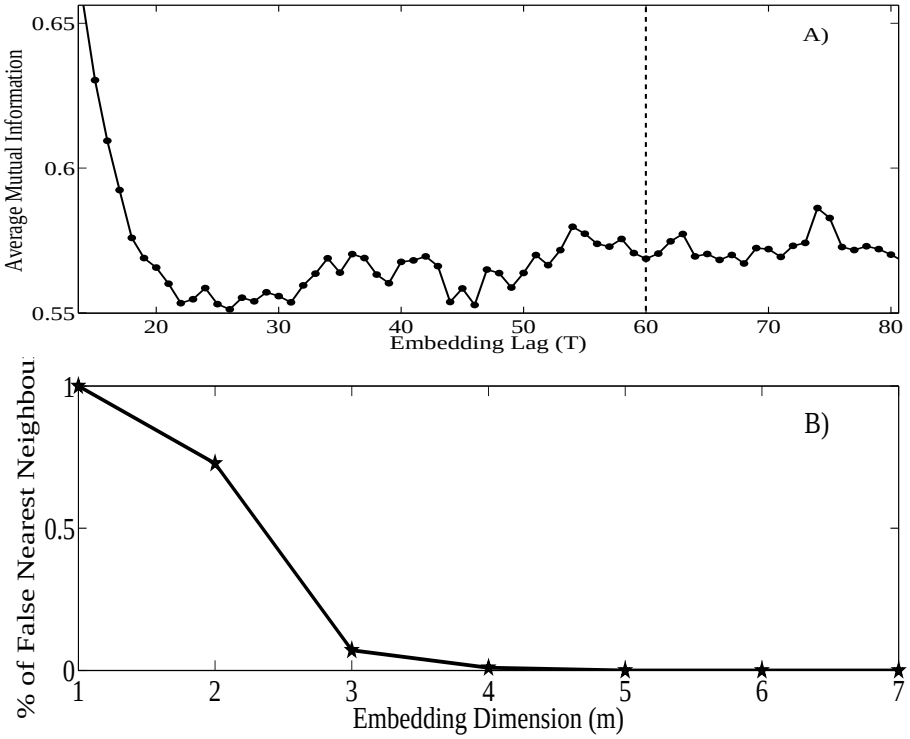

Figure 4: A) Average Mutual Information (AMI) and, B) False Nearest Neighbors (FNN). From these results, embedding lag and dimension are chosen to be $T = 60$ ms and $m = 4$, respectively.

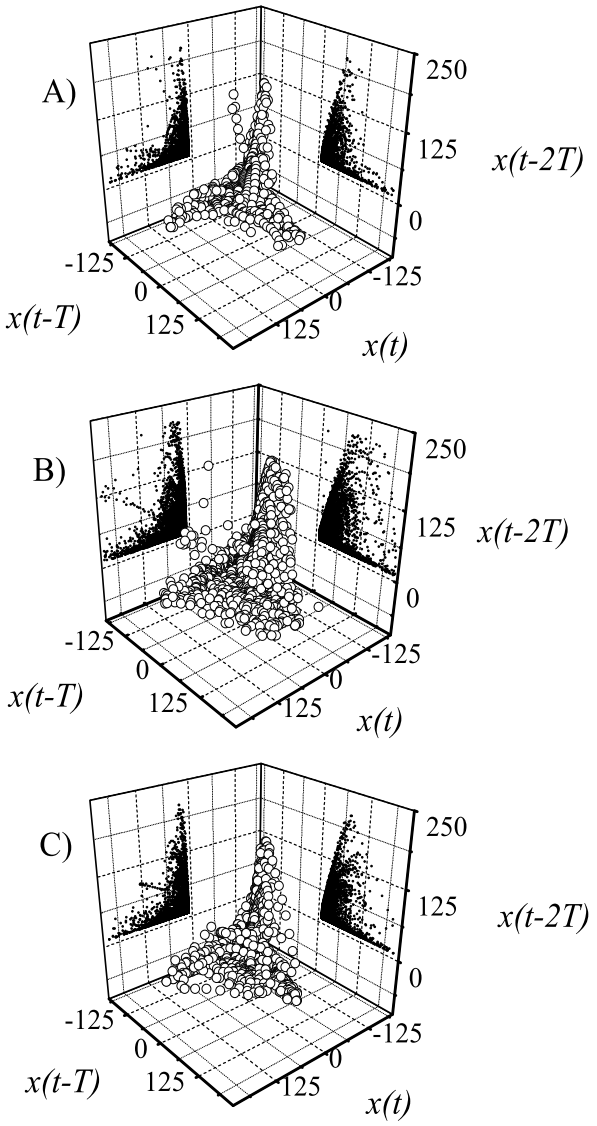

Figure 5: Phase space reconstruction of time series in Figure 3 A), B) and C), respectively. The phase space reconstruction show that all trajectories are contained in a bounded subspace, that means, the trajectories lie on an attractor.

3.2. Power spectrum

The power spectrum provides information about energy distribution at the fundamental frequencies of a system with oscillatory behavior. In the case of time series of Figure 3, the power spectra were computed via Fast Fourier Transform (FFT) [41]. The resulting power spectra are shown in Figure 6 where is possible to observe that there is not any dominant frequency. As a matter of fact, power spectrum is spread and it is rich at many frequencies giving an indicative of many components in oscillatory behavior. This result might be very important in studying synchronization of active cells releasing catecholamine molecules. In the light of spread spectrum results, synchrony of neurotransmission involves wide range of frequency components.

Note that the power spectrum in Figure 6A contains frequencies in a wider interval than those in figures 6B and 6C. This fact suggests that the frequencies interval is not identical among cells, corresponding to a real non-constant interval of spikes emergence. Thus, for instance, the frequency interval in Figure 6A is at least twice the interval in the others but energy is half. This reinforce the conjecture that exocytotic events in single chromaffin cells are structured but unpredictable and, chaotic behavior are expected. Next, an estimation of Maximum Lyapunov Exponent is computed to corroborate the conjecture.

3.3. Maximum Lyapunov Exponent

The time series dynamics has shown the existence of an embedding phase space as well as an attractive bounded subspace where the trajectories lies. These facts show a first sign of existence of nonlinear structure and possible existence of chaotic behavior. Nevertheless, it is necessary to study in depth more specific features in order to identify possible deterministic features. The typical features are the called empirical invariant measurements, such as entropies, Lyapunov exponents, equations of motion, etc. [42]. In this contribution, we explore the Lyapunov exponents measure, specifically the Maximum Lyapunow Exponent (MLE), because it can be computed with high accuracy. So, the spatial evolution of the system's trajectories was analyzed via computation of mean average of MLE. This parameter give us an estimation of trajectories divergence in oscillatory behavior.

The numerical value of the MLE defines the possible logarithmic separation of trajectories in the phase space of the system. By this reason, a positive MLE value is sufficient condition of existence of chaos behavior [43]. In the case of time series of adrenaline secretion in Figure 3, the MLEs were computed using the algorithm reported by Wolf et al. [44]. We compute the MLE at considering a specific orbit time ($EVOLV = 0.5$) and in defined set of spatial separation of fiducial points in phase space, $SCALMX \in (2, 4)$. The dark-solid lines in Figure 7 A), B) and C) show the MLE evolution of the trajectories of each attractor in Figure 5. The plots show that, in all cases, MLE evolution has an asymptotic behavior and holds in a positive value.

Because of the experimental nature of time series of catecholamine secretion, it is necessary to verify that positiveness of MLE are not due to the inherent

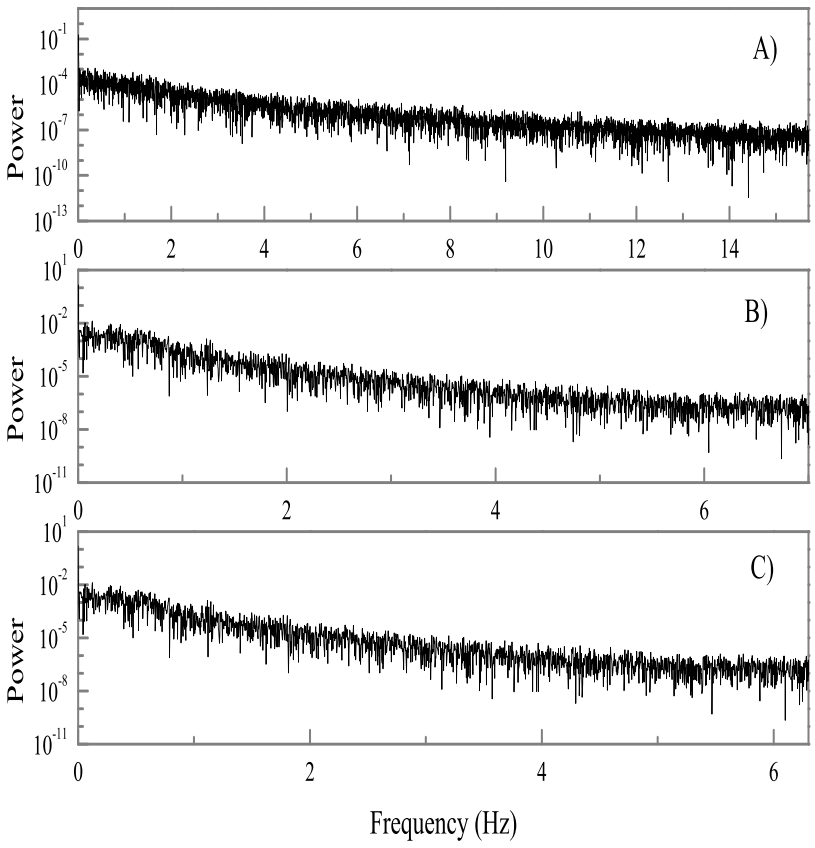

Figure 6: Power spectrum for the time series in Figure 3 A), B) and C), respectively. Note the corresponding differences in frequency scale.

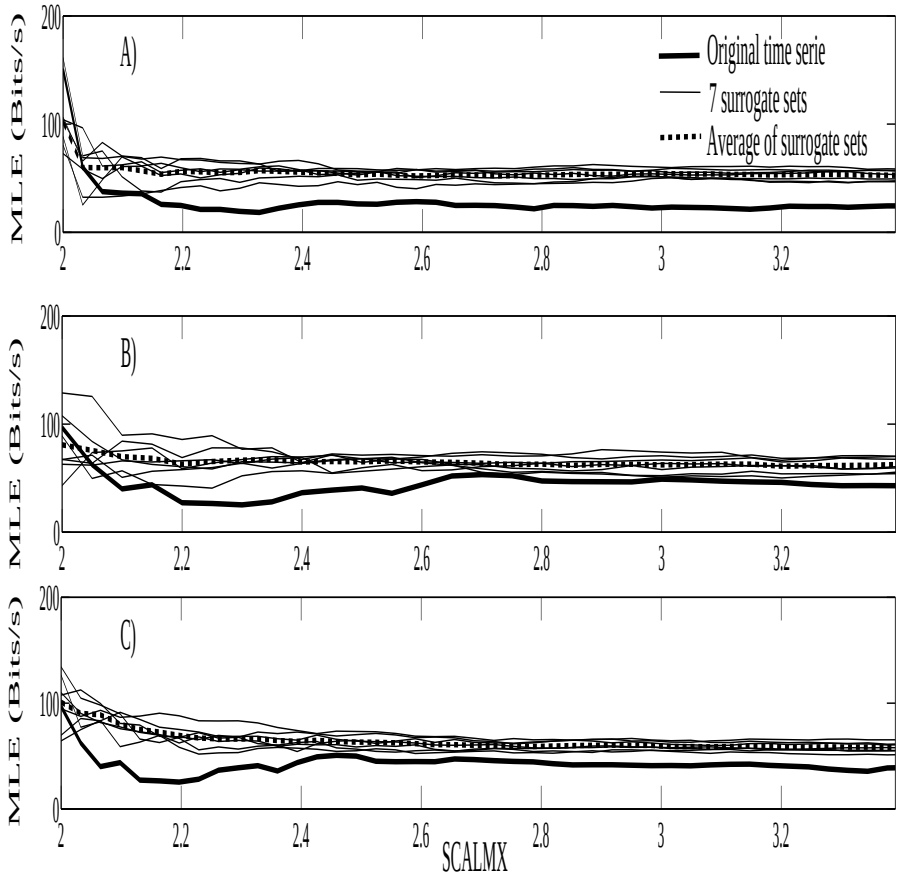

Figure 7: Maximum Lyapunov Exponent (MLE) evolution considering variations in maximum scale and orbit time. Dark-solid lines show the MLE of the original time series (raw data) in Figure 3 A, B and A. Solid lines show the MLE of each of the seven surrogate data set generated by the AAFT algorithm [**?**], and and preserving the Fourier spectrum of the raw data. Dark-dashed lines shows the mean-value trajectory of the MLE evolution of the surrogate sets for the three cases of study. In all cases, MLE evolution has an asymptotic behavior and holds in a positive value.

noise. By this reason, a statistical test based on surrogate data was carried out. The main goal of such approach is to generate a set of surrogate data which are consistent with the original time series (raw data). Basically, the surrogate data are randomly generated preserving a selected feature of the raw data [45]. In this study, we use the Amplitude Adjusted Fourier Transform (AAFT) algorithm reported by Kugiumtzis, 2000 [**?**], to generate seven surrogate data of each time series in Figure 3 and preserving Fourier spectrum of the raw data (see Figure 6).

After that, MLEs of each surrogate set are computed using the Wolf's algorithm, and considering the same simulation conditions that MLE calculation of original time series. Solid lines in Figure 7 show the seven MLE evolution of the surrogate data generated based on each of the three original time series. The dark-dashed lines show the mean-value trajectory of the MLE evolution of the seven surrogate sets. Similarly to the MLE evolution of the raw data, each one of the surrogate data has an asymptotic behavior, and holding in a positive value.

4. Concluding remarks

Measured data of catecholamine secretion in single mammal chromaffin cells were analyzed from a well-established experimental amperometry procedure. The resulting time series show the oscillatory behavior of catecholamine secretion during exocytosis process. The noise effects on the measurements are minimized ensuring that the assembly cell/liquid cleft/ultramicroelectrode used in amperometry behave as an artificial synapse guaranteeing the detection of the released catecholamine with high signal-to-noise ratio, as well as the determination of the instant released fluxes since the collection efficiency is quantitative. The ultramicroelectrode current mirrors precisely the released fluxes just selecting electrodes with a very stable amperometric baseline current. Furthermore, the signals of catecholamine secretion were designated as spikes if their maximum current values were 3 times higher than the RMS noise (0.5 to 0.7 pA) of the baseline current (30 ms minimum time-length) recorded prior to each signal. Also, special attention was applied to verify the baseline stability before and after each spike in order o avoid spike superimposition. These three facts ensure amperometric measurements with a high signal-to-noise ratio, implying that catecholamine secretion observed by means of amperometry is not a process governed by noise. Also, the absence of noise and effect of initial conditions (stationarity) suggests us the nonlinear behavior plagued of complexity. The high signal-to-noise ratio ensured by amperometric technique implies a first evidence of high irregularities in dynamics of time series in Figure 3, and such behavior could not be attributed to noise or uncertainties in cell process, but to a possible nonlinear characteristic of catecholamine secretion process.

The study of conventional techniques on time series analysis are used in order to elucidate if the evident irregularities showed in Figure 3 can be related to possible nonlinear dynamic in catecholamine secretion. The presented analysis

begins with the phase space reconstruction in order to seek for bounded attractors in the reconstructed phase space. AMI and FNN are computed to suggest embedding lag and embedding dimension of the reconstructed phase space. Figure 4 shows the values for embedding lag and embedding dimension, $T = 60$ ms and $m = 4$, respectively. The reconstructed attractors (Figure 5) can establish that, in all cases, the trajectories lie in a bounded embedding subspace. This fact shows that the trajectories are not disperse in the whole phase space but in a delimited area, inferring the existence of an attractor, and structured disorder in the system's dynamics.

The evidence of trajectories lying in embedding subspace of the reconstructed phase space is agree with the power spectra analysis which shows that there is not a dominant frequency of energy accumulation but spread spectra (Figure 6). Such dispersion allows us to conjecture a complex behavior, possibly chaotic, in the catecholamine secretion. Considering these results on structured oscillation and complex behavior, we analyze the MLE evolution for a given orbit time and a range of maximum scale (Figure 7). The MLE holds positive along the established range variation of orbit time and maximum scale. Moreover, the computation of the MLE of seven surrogate data sets guarantees that the positiveness of MLE are not due to experimental noise, and provides a strong indicator of chaotic behavior in catecholamine secretion. Such evidence give us elements to consider this phenomenon as an structured disorder; nevertheless, it is necessary more research in order to guarantee if the chaotic nature of catecholamine secretion is deterministic or stochastic.

In this contribution, we study elementary elementary knowledge of the nonlinear nature of catecholamine secretion and its dynamical features, these results establish a precedent for the complete characterization of the empirical invariant measurements of the embedding space where each attractor lies, towards a better understanding of the dynamical behavior of this phenomenon with the final intention of developing nonlinear models able to reproduce the behavior of catecholamine secretion in single mammal chromaffin cells.

References

[1] S.D. Shah, T.F. Clutter, P.E. Cryer, The human sympathochromaffin system, American Journal of Physiology 247 (1984) E380.

[2] P. Felig, L.A. Frohman, Endocrinology and metabolism, Fourth Edition, McGrawHill, USA, 2001.

[3] T.C. Sudhof, The synaptic vesicle cycle, Annu. Rev. Neurosci 27 (2004) 509.

[4] Y. Wang, B.L. Tang, SNAREs in neurons - beyond synaptic vesicle exocytosis, Mol, Memb. Biol. 23 (2006) 377.

[5] J. Lieberman, The ABCs of granue-mediated cytotoxicity: New weapons in the artesanal, Nat. Rev. Immunol. 3 (2003) 361.

[6] W.J. Hong, Cytotoxic T lymphocyte exocytosis: brig on the SNAREs, Trends Cell Biol. 15 (2005) 644.

[7] R.D. Burgoyne, A. Morgan, Secretory granule exocytosis, Physiol. Rev. 83 (2003) 581-632.

[8] S. An, D. Zenisek, Regulation of exocytosis in neurons and neuroendocrine cells, Curr. Opin. Neurobiol. 14 (2004) 522.

[9] W.E. Clutter, D.M. Bier, S.D. Shah, P.E. Cryer, Epinephrine plasma metabolic clearance rates and physiologic thresholds for metabolic and hemodynamic actions in man, Journal of Clinical Investigation 66 (1980) 94-101.

[10] H. Meiri, R. Rahamimoff, Clumping and oscillations in evoked transmitter release at the frog neuromuscular junction, Journal Physiology 278 (1978) 513-523.

[11] P.A. Pawson, A.D. Grinnell, Oscillation period of MEPP frequency at frog neuromuscular junctions is inversely correlated with release efficacy and independent of acute Ca^{2+} loading, Proceedings of the Royal Society B 237 (1989) 489-499.

[12] M.E. Kriebel, D.J. Bridy, Dynamics of ethanol-induced transmitter release in the frog neurotransmitter release junction, Brain Research 729 (1996) 228-233.

[13] S.B. Lowen, S.S. Casg, M. Poo, M.C. Teich, Quantal neurotransmitter secretion rate exhibits fractal behavior, Journal of Neurosciences 17 (1997) 5666-5677.

[14] N. Melamed, P.J. Helm, R. Rahamimoff, Confocal microscopy reveals coordinated calcium fluctuations and oscillations in synaptic boutons, Journal of Neuroscience 13 (1993) 632-649.

[15] W. Van der Kloot, I. Andricioaei, O.P. Balezina, Examining the timing of miniature endplate potential releases at the frog and mouse neuromuscular junctions for deviations from Poisson expectations, Pflug Archives: European Journal of Physiology 438 (1999) 578-586.

[16] I. Llano, J. Gonzalez, C. Caputo, F.A. Lai, L.M. Blayney, Y.P. Tan, A. Marty, Presynaptic calcium stores underlie large amplitud miniature IPSCs and spontaneous calcium transients, Nature Neuroscience 3 (2000) 1256-1265.

[17] N.J. Emptage, C.A. Reid, A. Fine, Calcium stores in hippocampal synaptic boutons mediate short-term plasticity, store-operated Ca^{2+} entry, and spontaneous transmitter release, Neuron 29 (2001) 197-208.

[18] C.R. Simkus, C. Stricker, The contribution of intracellular calcium stores to mEPSCs recorded in Layer II neurones of rat barrel cortex, Journal of Physiology 545 (2002), 521-535.

[19] T. Collin, A. Marty, I. Llano, Presynaptic calcium stores and synaptic transmission, Current Opinion of Neurobiology 15 (2005) 275-281.

[20] R.N. Leao, F.N. Leao, B. Walmsley, Non-random nature of spontaneous mIPSCs in mouse auditory brainstem neurons revealed by recurrence quantification analysis, Proceedings of the Royan Society B 272 (2005) 2551-2559.

[21] C. Amatore, Y. Bouret, L. Midrier, Time-resolved dynamics of the vesicle membrane during individual exocytotic secretion events, as extracted from amperometric monitoring of adrenaline exocytosis from chromaffin cells, Chemistry - A European Journal 5 (1999) 2151-2162.

[22] C. Amatore, B. Fosset, J. Bartelt, M.R. Deakin, R.M. Wightman, Electrochemical kinetics at microelectrodes: Part V. Migrational effects on steady or quasi-steady-state voltammograms, Journal of Electroanalytical Chemistry and Interfacial Electrochemistry 256 (1988) 255-268.

[23] T.J. Schroeder, J.A. Jankowski, K.T. Kawagoe, R.M. Wightman, C. Lefrou, C. Amatore, Analysis of Diffusional Broadening of Vesicular Packets of Catecholamines Released from Biological Cells During Exocytosis. Anal. Chemestry 64 (1992) 3077-3083.

[24] C. Amatore, Y. Bouret, E.R. Travis, R.M. Wightman, Adrenaline release by chromaffin cells: constrained swelling of the vesicle matrix leads to full fusion, Angewandte Chemie International Edition 29 (2000), 1952-1955.

[25] J.M. Finnegan, K. Pihel, P.S. Cahill, L. Huang, S.E. Zerby, A.G. Ewing, R.T. Kennedy, R.M. Wightman, Vesicular quantal sizemeasured by amperometry at chromaffin, mast, pheochromocytoma, and pancreatic beta-cells, Journal of Neurochemistry 66 (1996) 1914-1923.

[26] C. Amatore, S. Arbault, D. Bruce, P. de Oliveira, M. Erard, M. Vuillaume, Analysis of individual biochemical events based on artificial synapses using ultramicroelectrodes: cellular oxidative burst, Faraday Discuss (2000) 319-333.

[27] S.F. Dressman, J.L. Peters, A.C. Michael, Carbon fiber microelectrodes with multiple sensing elements for in vivo voltammetry, Journal of Neurosciences Methods 119 (2002) 75-81.

[28] K. Pihel, T.J. Schroeder, R.M. Wightman, Rapid and selective cyclic voltammetric measurements of epinephrine and norepinephrine as a method to measure secretion from single bovine adrenal medullary cells, Analytical Chemistry 66 (1994) 4532-4537.

[29] R.M. Wightman, J.A. Jankowski, R.T. Kennedy, K.T. Kawagoe, T.J. Schroeder, D.J. Leszczyszyn, J.A. Near, E.J. Diliberto, O.H. Viveros, Resolved catecholamine spikes correspond to single vesicle release from individual chromaffin cells, The Proceedings of the National Academy of Sciences U.S.A. 88 (1991) 10754-10758.

[30] B.G. Livett, Adrenal-medullary chromaffin cells-in vitro, Physiological Reviews 64 (1984) 1103-1161.

[31] S. Arbault, P. Pantano, J.A. Jankowski, M. Vuillaume, C. Amatore, Monitoring an oxidative stress mechanism at a single human fibroblast, Analytical Chemistry 67 (1995) 3382-3390.

[32] N.H. Packard, J.P. Crutchfield, J.D. Farmer, R.S. Shaw, Geometry from a time series, Physics Review Letters, 45 (1980) 712.

[33] F. Takens, Detecting strange attractors in turbulence, Springer, Berlin, 1981.

[34] H. Kantz, T. Schreiber, Nonlinear Time Series Analysis, Cambridge University Press, UK, 2004.

[35] M. Small, Applied nonlinear time series analysis: Applications in physics, physiology and finance, World Scientific, Singapore, 2005.

[36] H.D.I. Abarbanel, Analysis of observed chaotic data, Springer-Verlag, New York, USA, 1996.

[37] M. Perc, The dynamics of human gait, European Journal of Physics 26 (2005) 525-534.

[38] M. Perc, Nonlinear time series analysis of the human electrocardiogram, European Journal of Physics 26 (2005) 757-768.

[39] S. Kodba, M. Perc, M. Marhl, Detecting chaos from time series, European Journal of Physics 26 (2005) 205-215.

[40] B. Krese, M. Perc, E. Govekar, The dynamics of laser droplet generation, Chaos 20 (2010) 013129.

[41] R. Femat, J. Alvarez-Ramirez, A. Soria, Chaotic flow structure in a vertical bubble column, Physics Letters A 248 (1998) 67-79.

[42] H. Kantz, Time series analysis in reconstructed state spaces, Stochastics and Dynamics 1 (2001) 85-111.

[43] J.P. Eckmann, D. Ruelle, Ergodic theory of chaos and strange attractors, Reviews of Modern Physics 57 (1985) 617.

[44] A. Wolf, J.B. Swift, H.L. Swinney, J.A. Vastano, Determining Lyapunov exponents from a time series, Physics D 16 (1985) 285-317.

[45] J. Theiler, F. Eubank, A. Longtin, B. Galdrikian, J.D. Farmer, Testing for nonlinearity in time series: a method of surrogate data, Physica D 58 (1992) 77-94.

[46] D. Kugiumtzis, Surrogate data test for nonlinearity including nonmonotinic transforms, Physical Review E 62 (2000) R25-R28.